Supporting Information

Highly Efficient Tin Perovskite Solar Cells Achieved Under Wide Oxygen Region

Xin He,[ac] Tianhao Wu,[b] Xiao Liu,[a] Yanbo Wang,[b] Xiangyue Meng,[a] Jihuai Wu,[*c] Takeshi Noda,[a] Xudong Yang,[b] Yutaka Moritomo,[d] Hiroshi Segawa,[e] and Liyuan Han[*a bd]

[a]*Photovoltaic Materials Group,Center for Green Research on Energy and Environmental Materials, National Institute for Materials Science, Tsukuba, Ibaraki 305-0047, Japan.*

[b]*State Key Laboratory of Metal Matrix Composites, Shanghai Jiao Tong University, 800 Dong Chuan Road, Shanghai 200240, China.*

[c]*Engineering Research Center of Environment-Friendly Functional Materials for Ministry of Education, Institute of Materials Physical Chemistry, Huaqiao University, 668 Jimei Avenue, Xiamen 361021, China.*

[d]*Faculty of Pure and Aplied Science, University of Tsukuba, Tsukuba, Ibaraki 305-8571, Japan*

[e]*Research Center for Advanced Science and Technology, The University of Tokyo, Tokyo 153-8904, Japan*

[*] Corresponding author. E-mail address: Han.liyuan@nims.go.jp; jhwu@hqu.edu.cn.

Materials

All the chemicals were used as received without any further purification. SnI_2 (99.99%, Sigma-Aldrich), SnF_2 (>99%, Sigma-Aldrich). $CH(NH_2)_2I$ (FAI) (>98%) and 4-Fluorobenzohydrazide (FBH) (>98%) were purchased from Tokyo Chemical Industry Co., Japan. Fullerene-C60 (99.95%), Bathocuproine (>99%), and super dehydrated solvent containing dimethyl sulfoxide (DMSO), chlorobenzene (CB) were purchased from Wako Co., Japan.

First-principle calculation

Geometry optimizations of the FBH molecule were performed on the Guassian 09 program by using B3LYP as the exchange-correlation function with all-electron double-ξ valence basis sets of 6-31G* based on the DFT methods. Vibrational frequency calculations were also used to make sure the optimized structures of the corresponding molecules have no imaginary frequency with default spin mode at the gas phase. For the simulation of oxygen-absorbed $FASnI_3$ and $FASnI_3$-FBH models, the generalized gradient approximation (GGA) with the Perdew-Burke-Ernzerhof (PBE) exchange correlation functional was used with norm-conserving pseudopotential for H atoms and the ultra-soft pseudopotentials for C, N, O, F, I, and Sn atoms in the spin-polarized DFT calculations,[1-3] and the plane-wave kinetic energy cutoff was fixed at 380 eV. Surface slabs were simulated as FA-terminated (100) slabs in the orthorhombic structure, which has three layers of $[SnI_6]^{4-}$ units in total. Moreover, about 25 Å vacuum space was introduced on the top of each slab surface to reduce the interaction between the adjacent layers.

The absorption energy (E_{abs}) of oxygen onto the $FASnI_3$ perovskite lattice was calculated by the equation $E_{abs} = E_f(FASnI_3\text{-}O_2) - [E_f(FASnI_3) + E_f(O_2)]$, where $E_f(FASnI_3\text{-}O_2)$, $E_f(FASnI_3)$ and $E_f(O_2)$ are the formation energy of the corresponding simulation models, and the E_{abs} for $FASnI_3$-FBH model was calculated based on the same method.

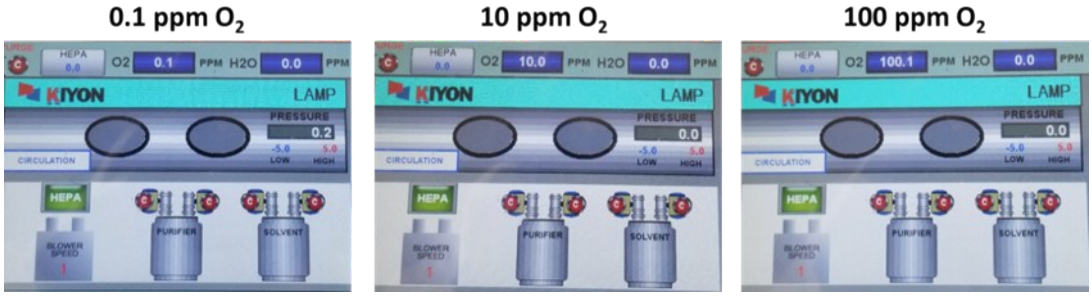

Fig. S1 The oxygen concentration of the film fabricated condition monitored by a digital detector in the glove box.

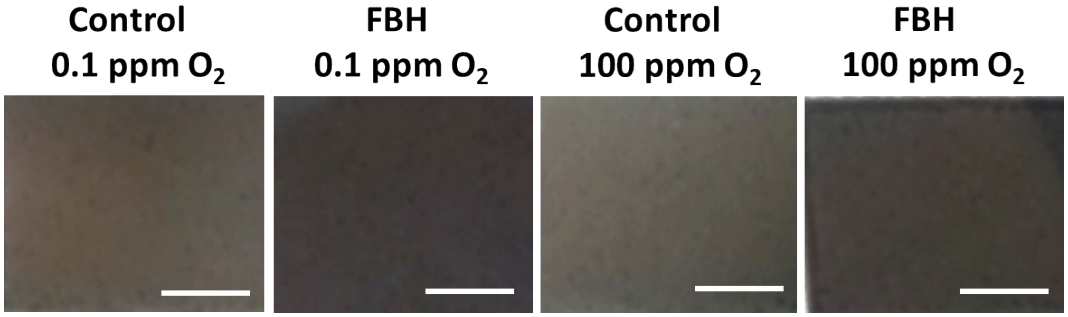

Fig. S2 The photographs of the as-preparing tin perovskite films fabricated at different oxygen conditions with a scale bar of 0.5 cm.

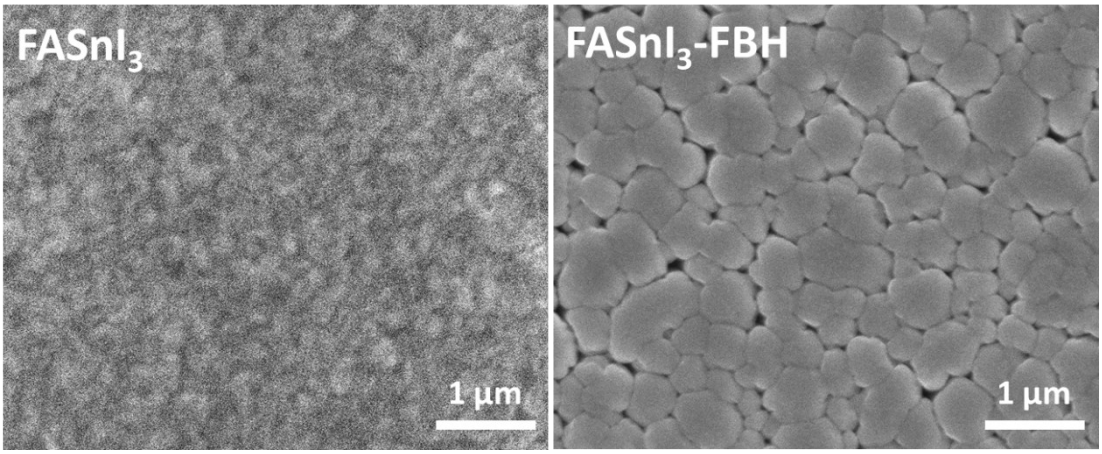

Fig. S3 The SEM morphology of the $FASnI_3$ perovskite films without or with FBH treatment fabricated at the normal oxygen condition before thermal annealing process.

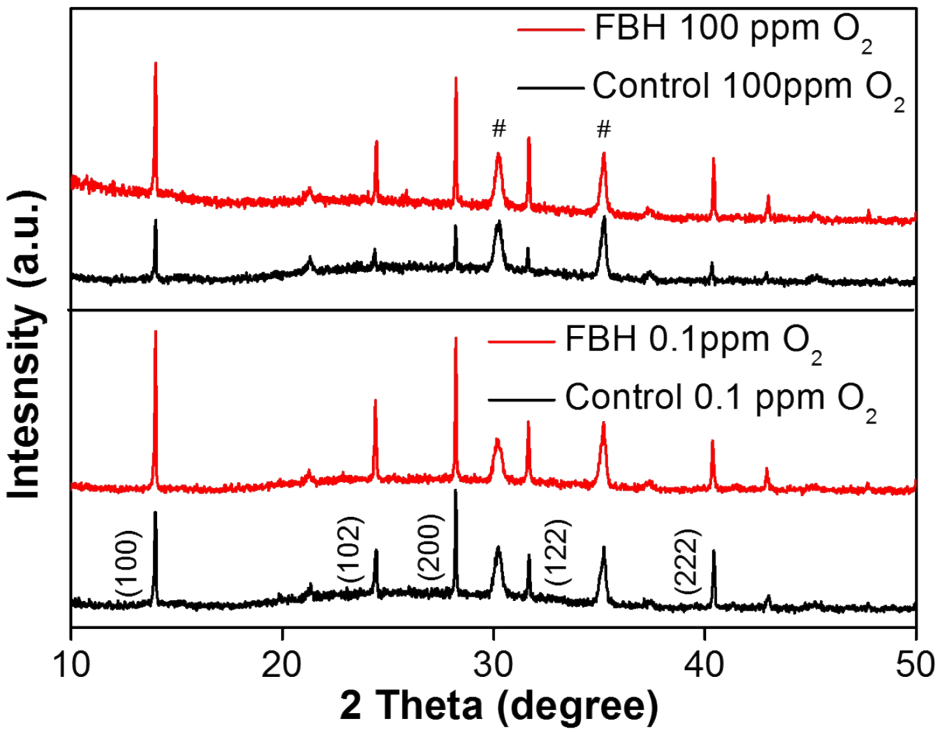

Fig. S4 XRD patterns of the $FASnI_3$ perovskite films treated with the antisolvent (chlorobenzene) without or with FBH molecules fabricated at the normal oxygen condition (0.1 ppm O_2) or the higher oxygen condition (100 ppm O_2). The symbol # represents the diffraction peaks of ITO glass.

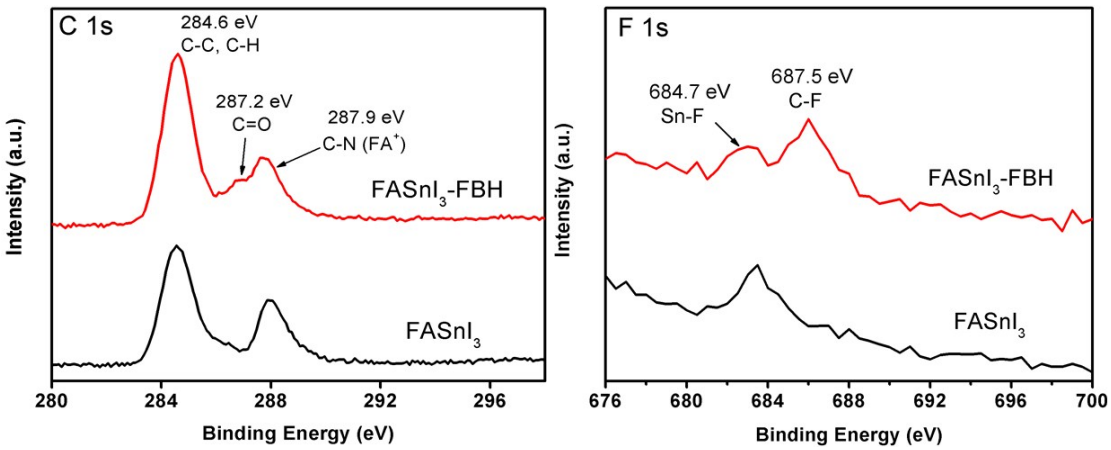

Fig. S5 XPS C 1s and F 1s spectrums of the $FASnI_3$ perovskite films before and after the FBH treatment.

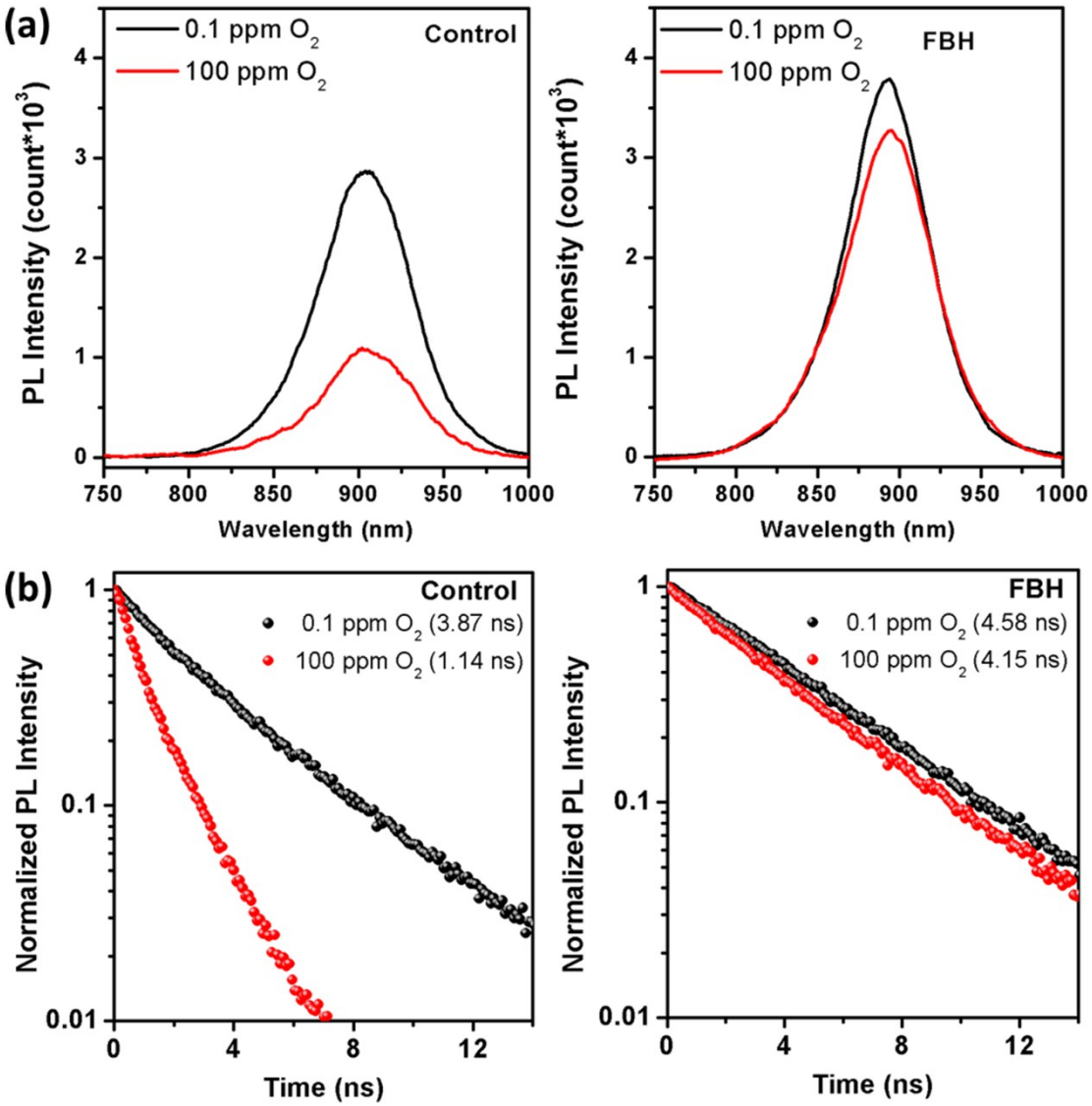

Fig. S6 a) Steady-state PL spectrums and b) time-resolved PL decay plots of the corresponding perovskite films. All the samples for PL measurement were deposited on the bare glass substrate.

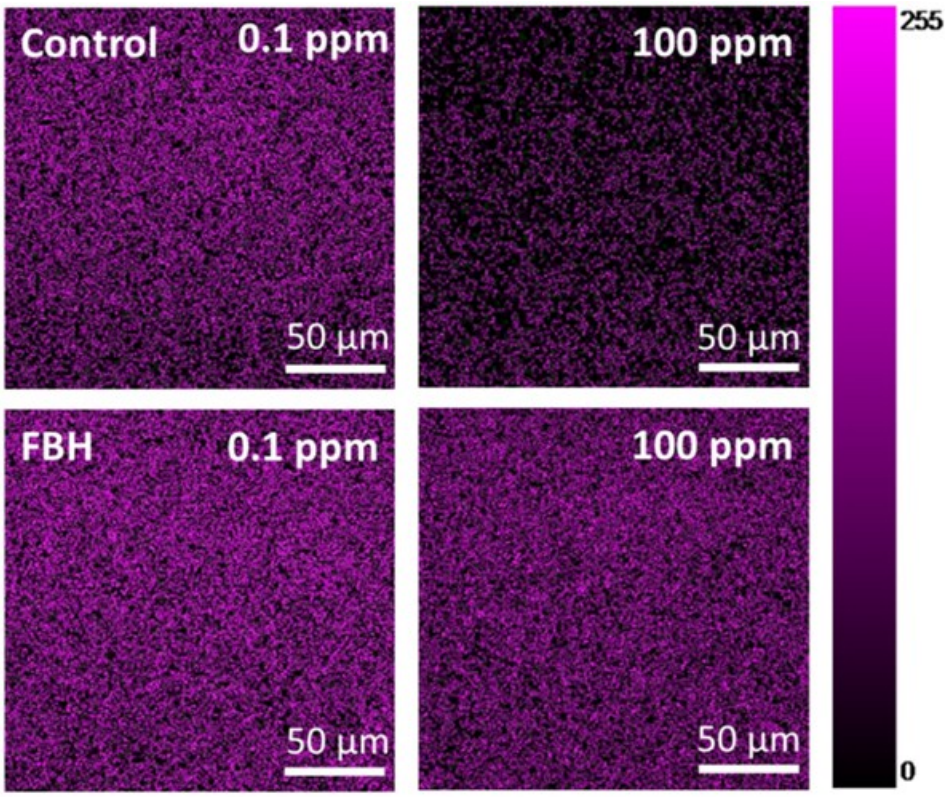

Fig. S7 Two-dimensional PL mapping by the confocal-fluorescence spectroscopy for the corresponding perovskite films fabricated at 0.1 ppm and 100 ppm oxygen concentration., the PL mapping area is 200 um × 200 um at the bare glass substrate.

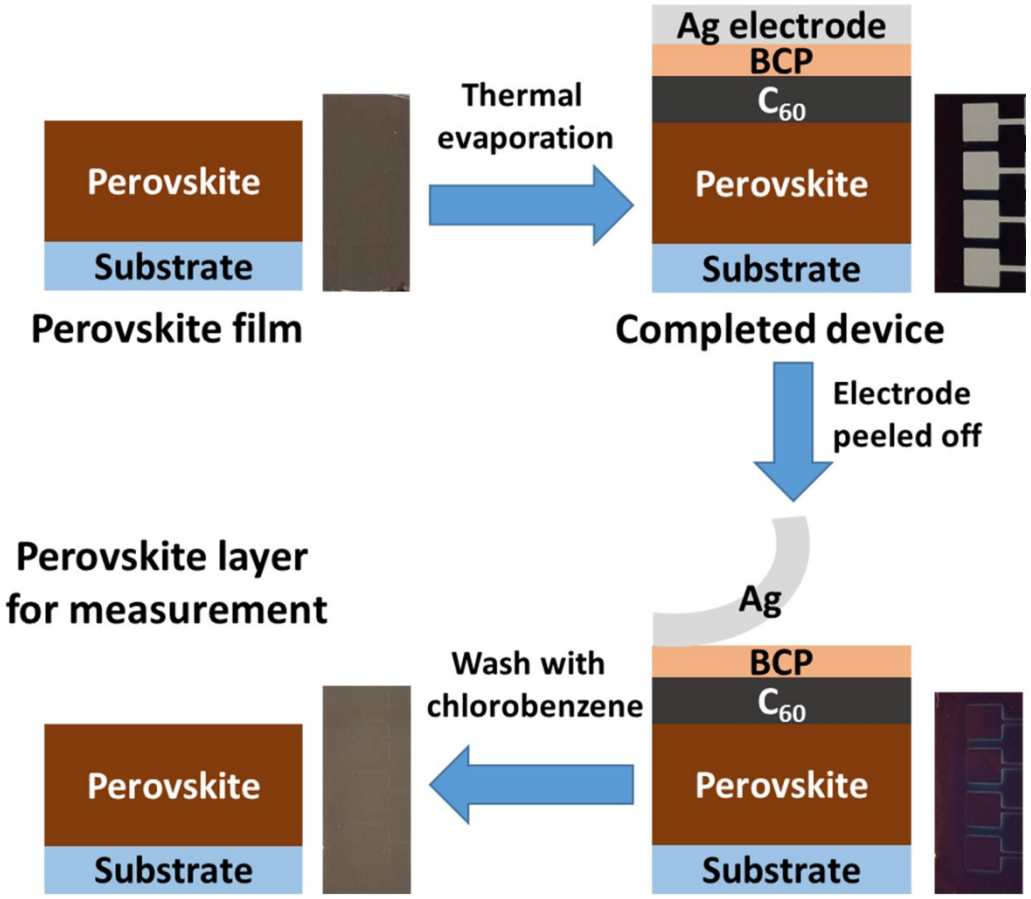

Fig. S8 Preparation of the perovskite sample of a completed device for the FTIR and XPS measurement, the insets show the top-view photo of the samples.

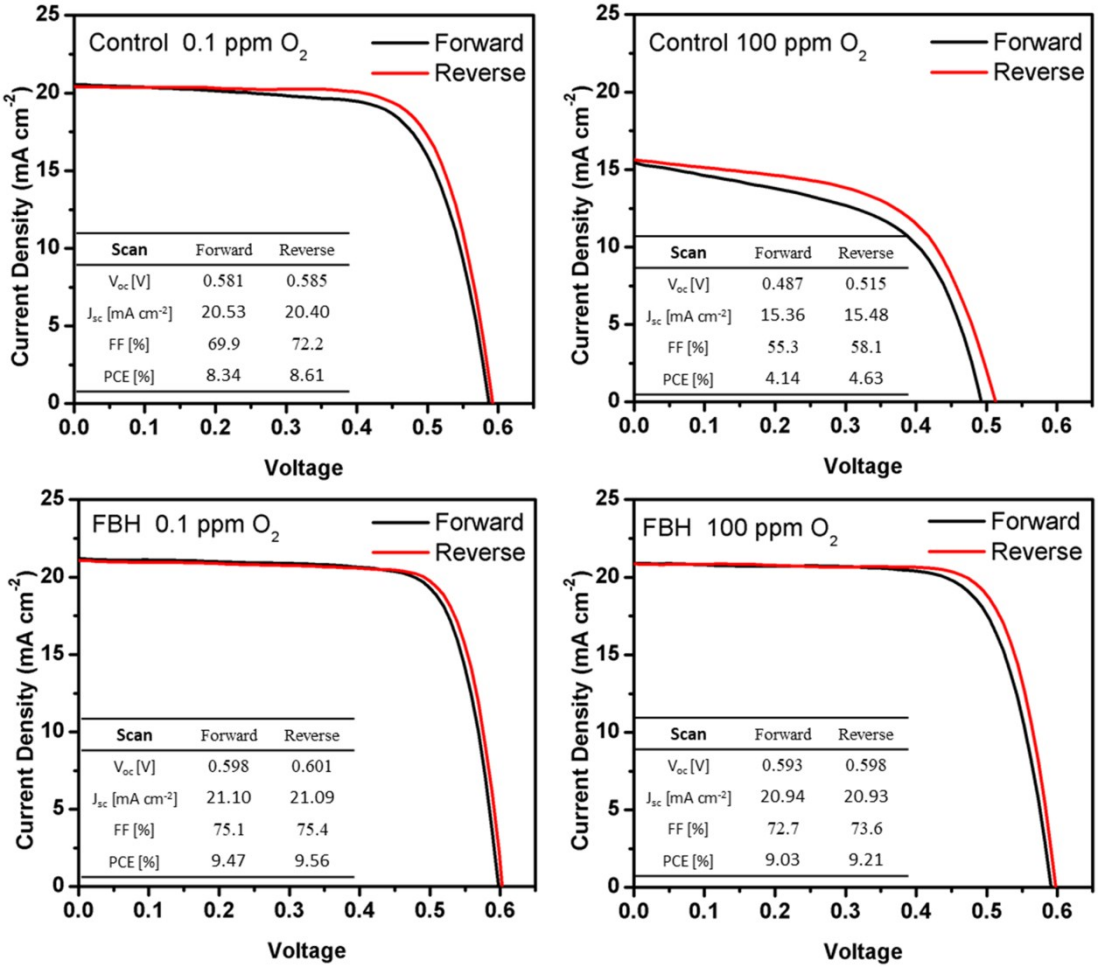

Fig. S9 The *J-V* hysteresis analysis of the corresponding tin perovskite solar cells.

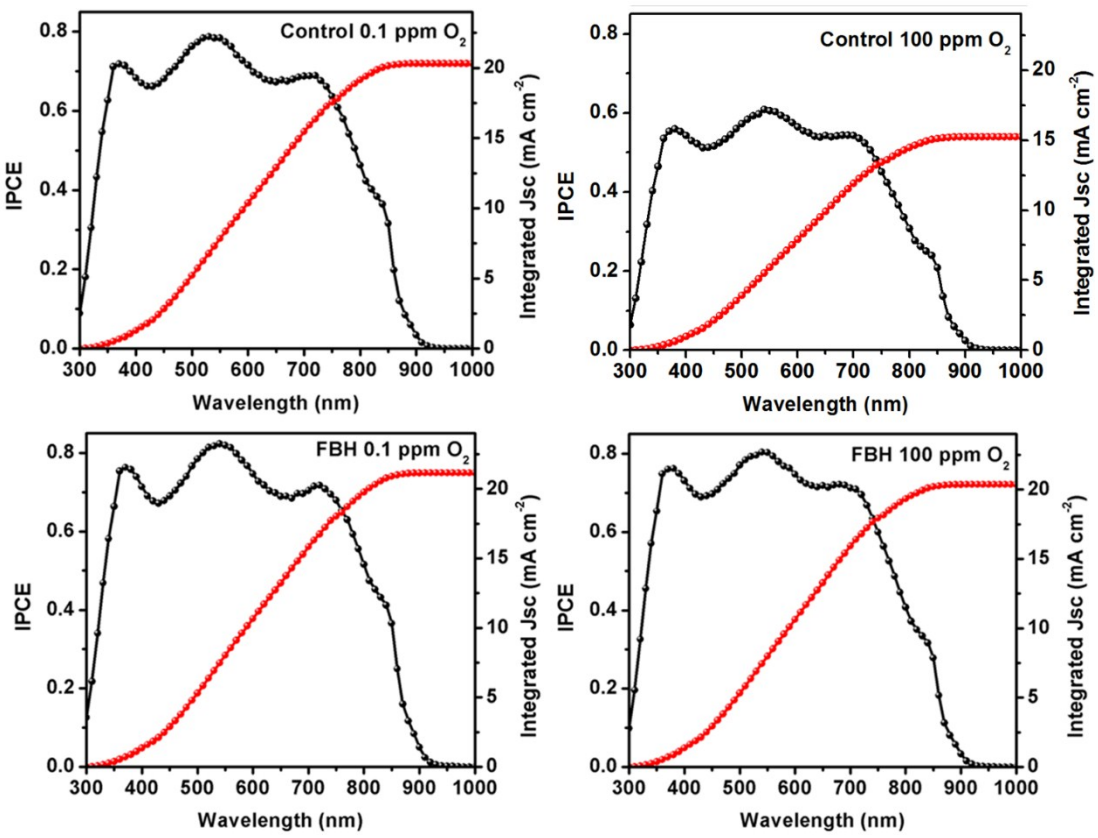

Fig. S10 Incident photon-to-current efficiency (IPCE) spectrums of the corresponding perovskite devices measured from 300 nm to 1000 nm.

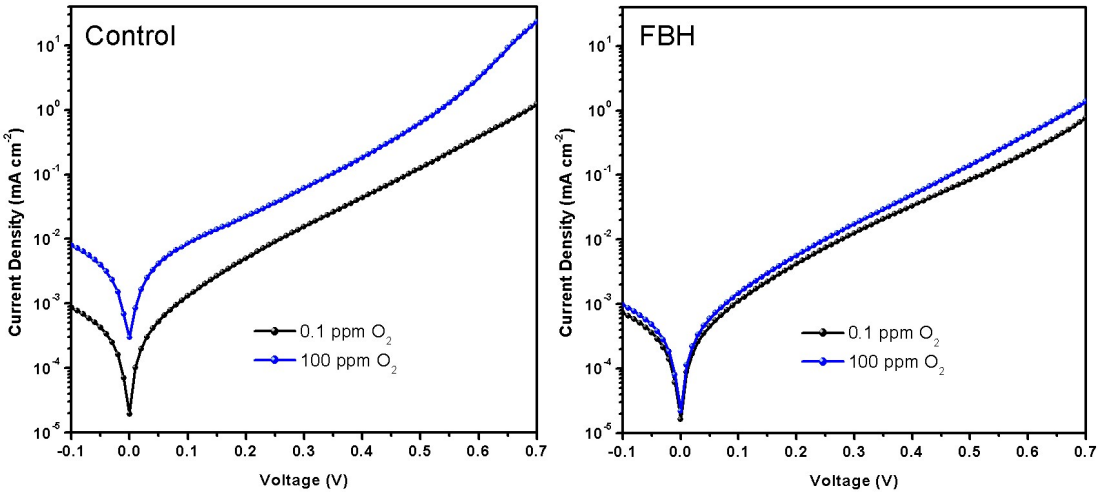

Fig. S11 Dark *J-V* plots of the corresponding TPSCs fabricated at the condition of 0.1 ppm oxygen and 100 ppm oxygen.

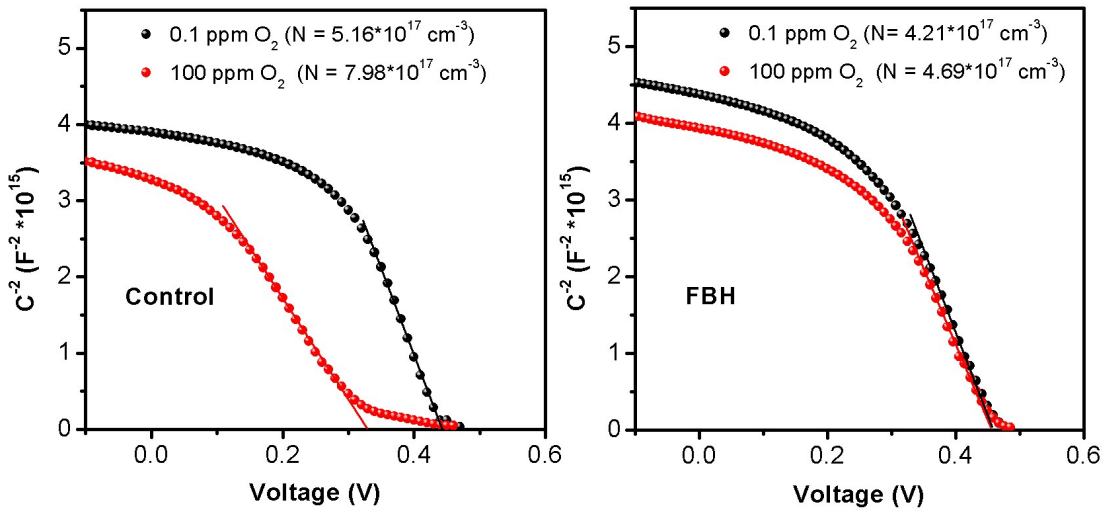

Fig. S12 Mott-Schottky analysis of the control and FBH-treated TPSCs fabricated at different oxygen condition.

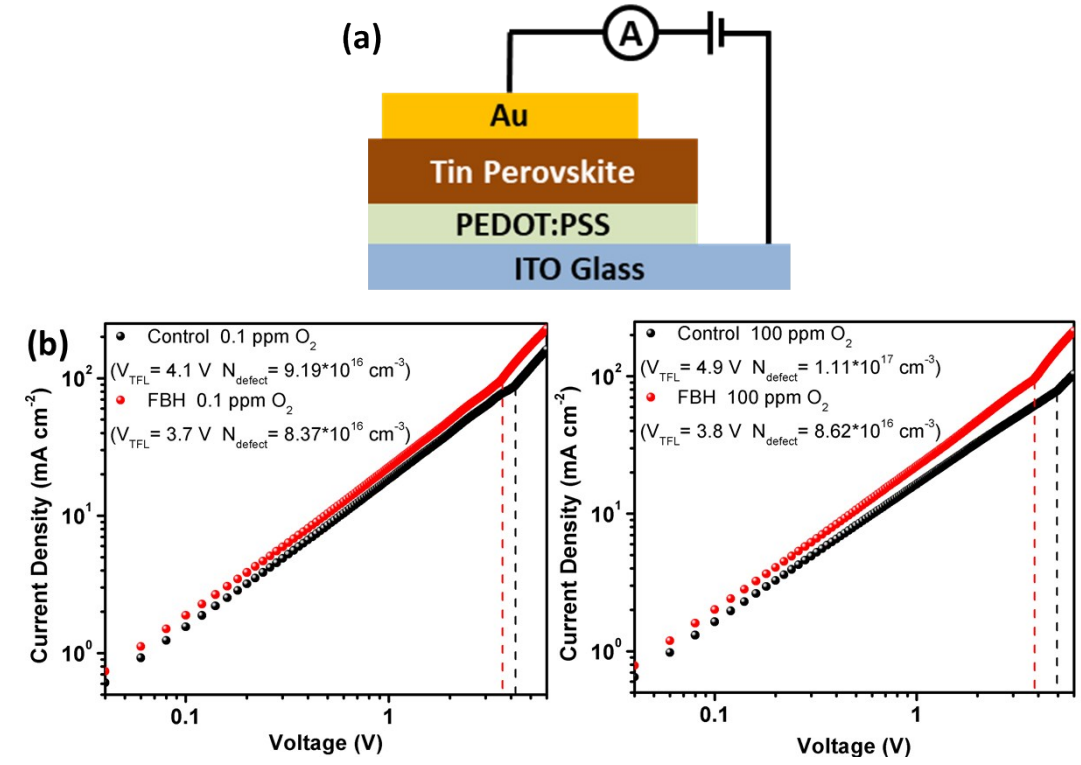

Fig. S13 (a) Device structure of the SCLC measurement. (b) Dark *J-V* curves of the devices fabricated at different oxygen conditions derived from the SCLC analysis.

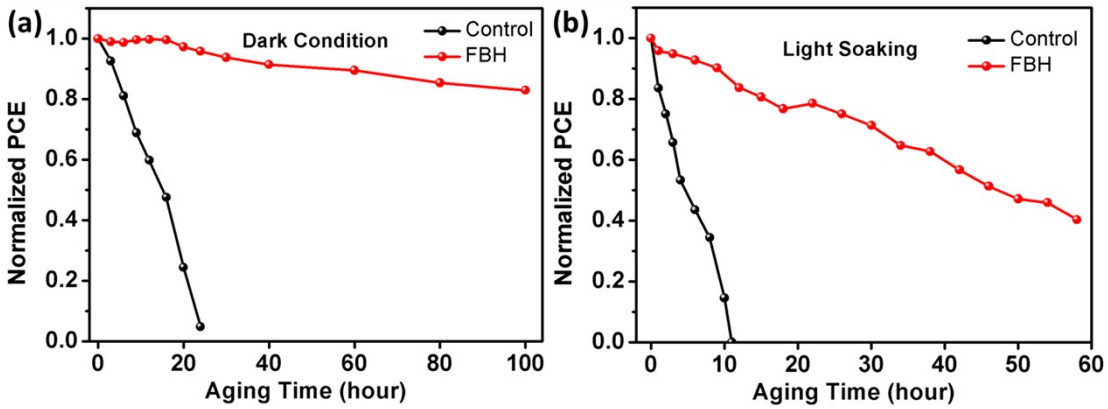

Fig. S14 The stability test of the TPSCs fabricated at 0.1 ppm oxygen measured under (a) dark and (b) light soaking conditions in ambient air with a relative humidity of 20%.

Table S1. The fitting data of PL decay plots for the corresponding perovskite film. Decay lifetime of the time-resolved PL analysis is calculated by the single-exponential decay equation: $y = Aexp(-t/\tau)$. Where y is the PL intensity, τ is the decay lifetime, and A is the independent constant.

Perovskite film	Oxygen Content	A value	A error	τ value [ns]	τ error [ns]
$FASnI_3$	0.1 ppm	0.91	0.0020	3.87	0.0024
	100 ppm	1.00	0.0025	1.14	0.0042
$FASnI_3$-FBH	0.1 ppm	1.04	0.0007	4.58	0.0065
	100 ppm	0.98	0.0009	4.15	0.0050

Table S2. Device parameter for pristine $FASnI_3$ and the $FASnI_3$-FBH based TPSCs

Perovskite	Oxygen Content	J_{SC} [mA cm^{-2}]	V_{OC} [V]	FF [%]	PCE [%]	PCE[a)] [%]
$FASnI_3$	0.1 ppm	20.53	0.581	69.9	8.34	8.02
	10 ppm	19.07	0.556	64.8	6.87	6.39
	100 ppm	15.36	0.487	55.3	4.14	3.30
$FASnI_3$-FBH	0.1 ppm	21.10	0.598	75.1	9.47	9.25
	10 ppm	20.98	0.597	74.5	9.33	9.08
	100 ppm	20.94	0.593	72.7	9.03	8.69

[a)]The average PCE for the TPSCs calculated based on 16 individual cells under forward scan.

Table S3. A summary of the detail photovoltaic parameters of highly efficient tin perovskite solar cells reported in the recent works.

Perovskite	Treatment	*V*oc [V]	*J*sc [mA cm^{-2}]	FF [%]	PCE [%]	Reference
$FASnI_3$	Additive engineering	0.61	21.2	72.9	9.56	Jokar et al. [4]
$FASnI_3$	Additive engineering	0.58	21.3	71.8	8.87	Jokar et al. [5]
$FASnI_3$	Additive engineering	0.52	24.1	71.0	8.89	Shao et al. [6]
$FASnI_3$	Additive engineering	0.61	22.0	70.1	9.41	Wang et al. [7]
$FASnI_3$	Additive engineering	0.56	23.2	72.6	9.44	Ran et al. [8]
$FASnI_3$	Additive engineering	0.61	20.1	68.6	8.49	Meng et al. [9]
$FASnI_3$	Interface engineering	0.56	22.8	74.0	9.37	Muhammad et al. [10]
$FASnI_3$	Solvent engineering	0.55	24.3	67.3	9.06	Liu et al. [11]
$FASnI_3$	Interface engineering	0.59	21.1	75.1	9.47	This work

References

1 G. Kresse and J. Furthmüller, *Phys. Rev. B*, 1996, **54**, 11169.

2 G. Kresse and J. Furthmüller, *Comp. Mater. Sci.*, 1996, **6**, 15-50.

3 C. Lee, W. Yang and R. G. Parr, *Phys. Rev. B*, 1988, **37**, 785.

4 E. Jokar, C. H. Chien, C. M. Tsai, A. Fathi and E. W. G. Diau, *Adv. Mater.*, 2019, **31**, 1804835.

5 E. Jokar, C. H. Chien, A. Fathi, M. Rameez, Y. H. Chang and E. W. G. Diau, *Energy Environ. Sci.*, 2018, **11**, 2353-2362.

6 S. Shao, J. Liu, G. Portale, H. H. Fang, G. R. Blake, G. H. ten Brink, L. J. A. Koster and M. A. Loi, *Adv. Energy Mater.*, 2018, **8**, 1702019.

7 F. Wang, X. Jiang, H. Chen, Y. Shang, H. Liu, J. Wei, W. Zhou, H. He, W. Liu and Z. Ning, *Joule*, 2018, **2**, 2732-2743.

8 C. Ran, W. Gao, J. Li, J. Xi, L. Li, J. Dai, Y. Yang, X. Gao, H. Dong and B. Jiao, *Joule*, 2019, 12, **3**, 1–16.

9 X. Meng, J. Lin, X. Liu, X. He, Y. Wang, T. Noda, T. Wu, X. Yang and L. Han, *Adv. Mater.*, 2019, **31**, 1903721.

10 M. A. Kamarudin, D. Hirotani, Z. Wang, K. Hamada, K. Nishimura, Q. Shen, T. Toyoda, S. Iikubo, T. Minemoto and K. Yoshino, *J. Phys. Chem. Lett.*, 2019, **10**, 5277-5283.

11 X. H. Liu, K. Yan, D. W. Tan, X. Liang, H. M. Zhang and W. Huang, *ACS Energy Lett.*, 2018, **3**, 2701-2707.